Resource Analysis of a Fault-Tolerant Quantum Computer

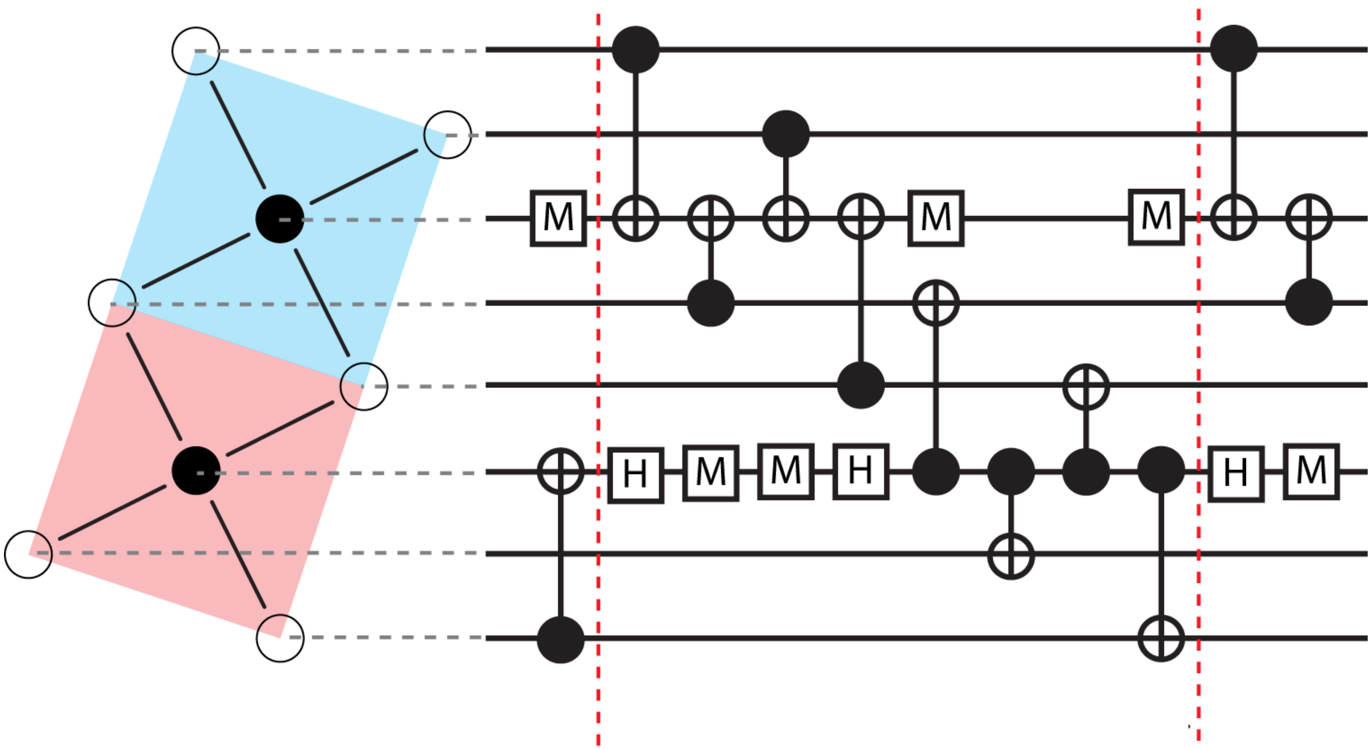

Yoshihisa Yamamoto, Cody Jones, Rodney Van Meter

最先端研究開発支援プログラム「量子情報処理プロジェクト」全体会議2011

（京都　2011年12月13-16日）

Problem Statement

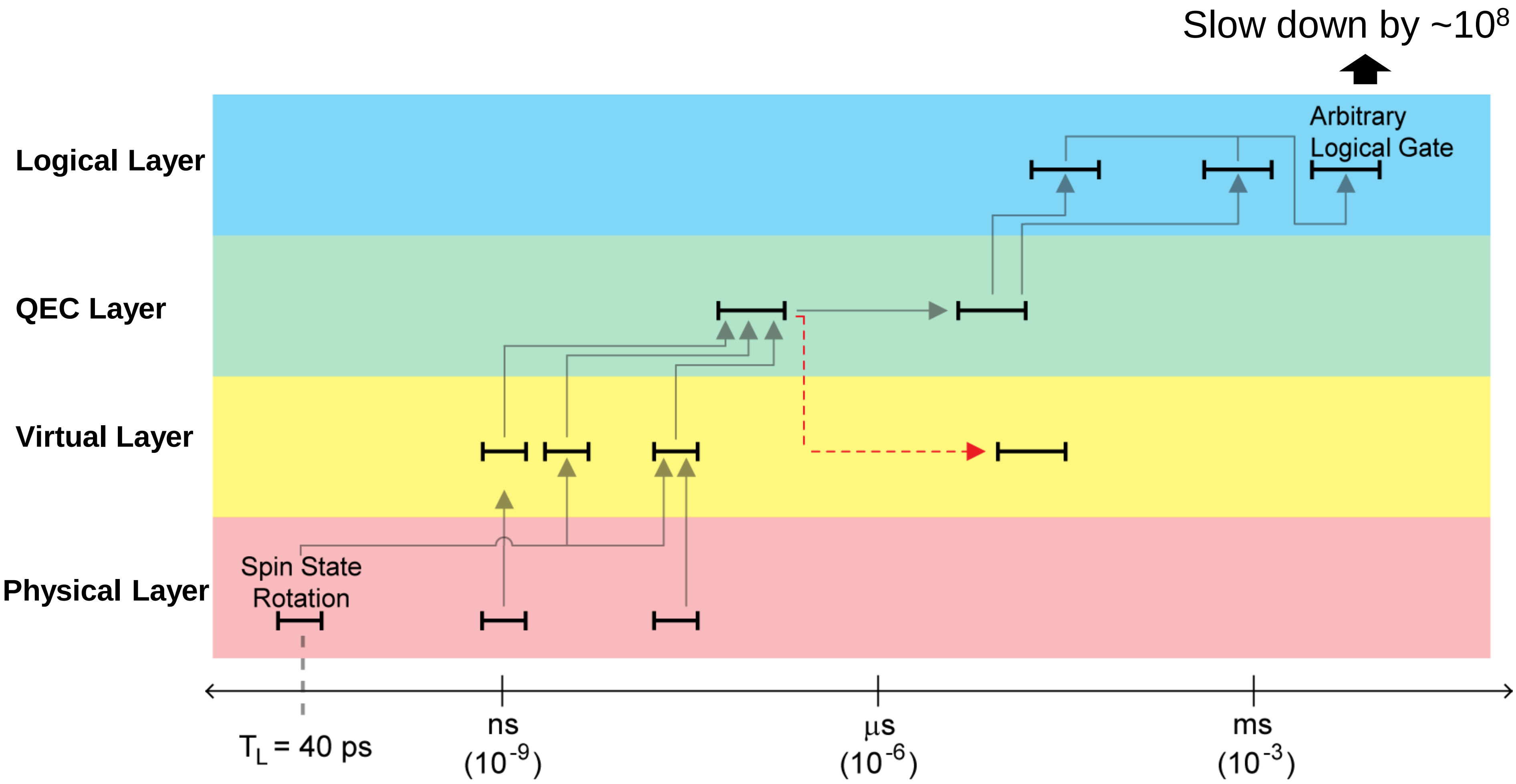

Optical control
of quantum dot spins

Physical Qubits

― Cavity QED Systems with Single-Electron-Doped Quantum Dots ―

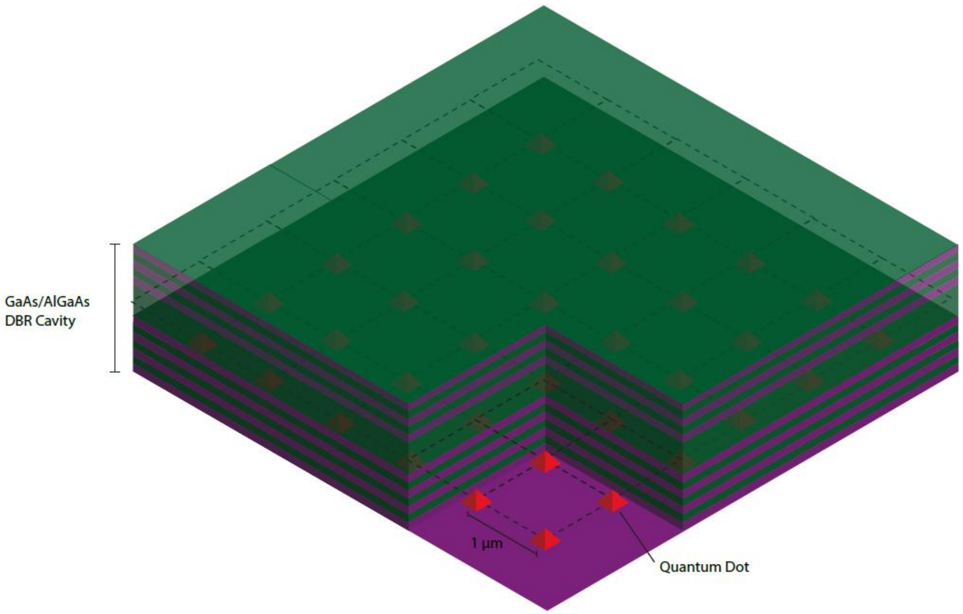

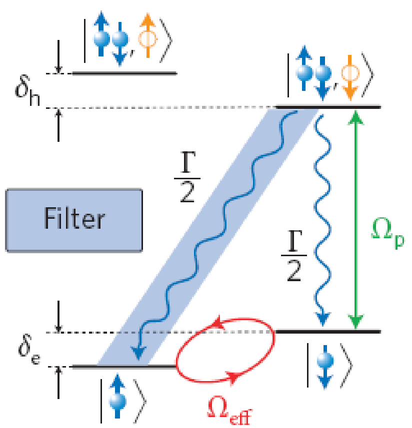

Layered architecture for quantum computing

N. Cody Jones, Rodney Van Meter, Austin G. Fowler, Peter L. McMahon, Jungsang Kim, Thaddeus D. Ladd, and Yoshihisa Yamamoto arXiv:1010.5022v2 [quant-ph] 5 Dec 2011

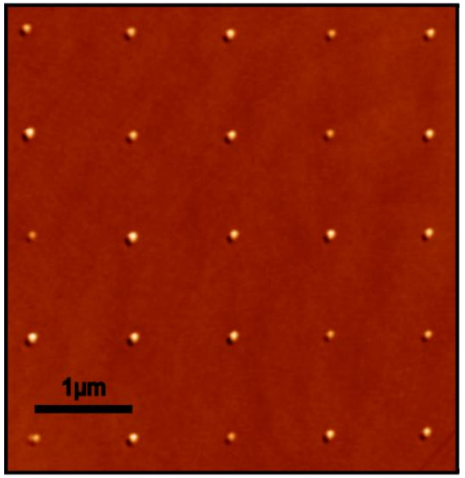

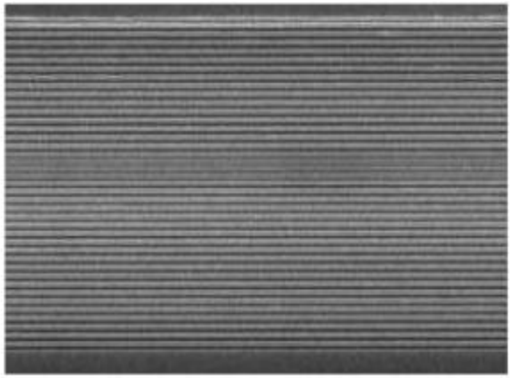

A simple planar microcavity with 2D lattice of site-controlled QDs

C. Schneider, M. Strauss, T. Sunner, A. Huggenberger, D. Wiener, S. Reitzenstein, M. Kamp, S. Höfling and A. Forchel *APL* 92, 183101 (2008)

Primary Components of the Physical Layer

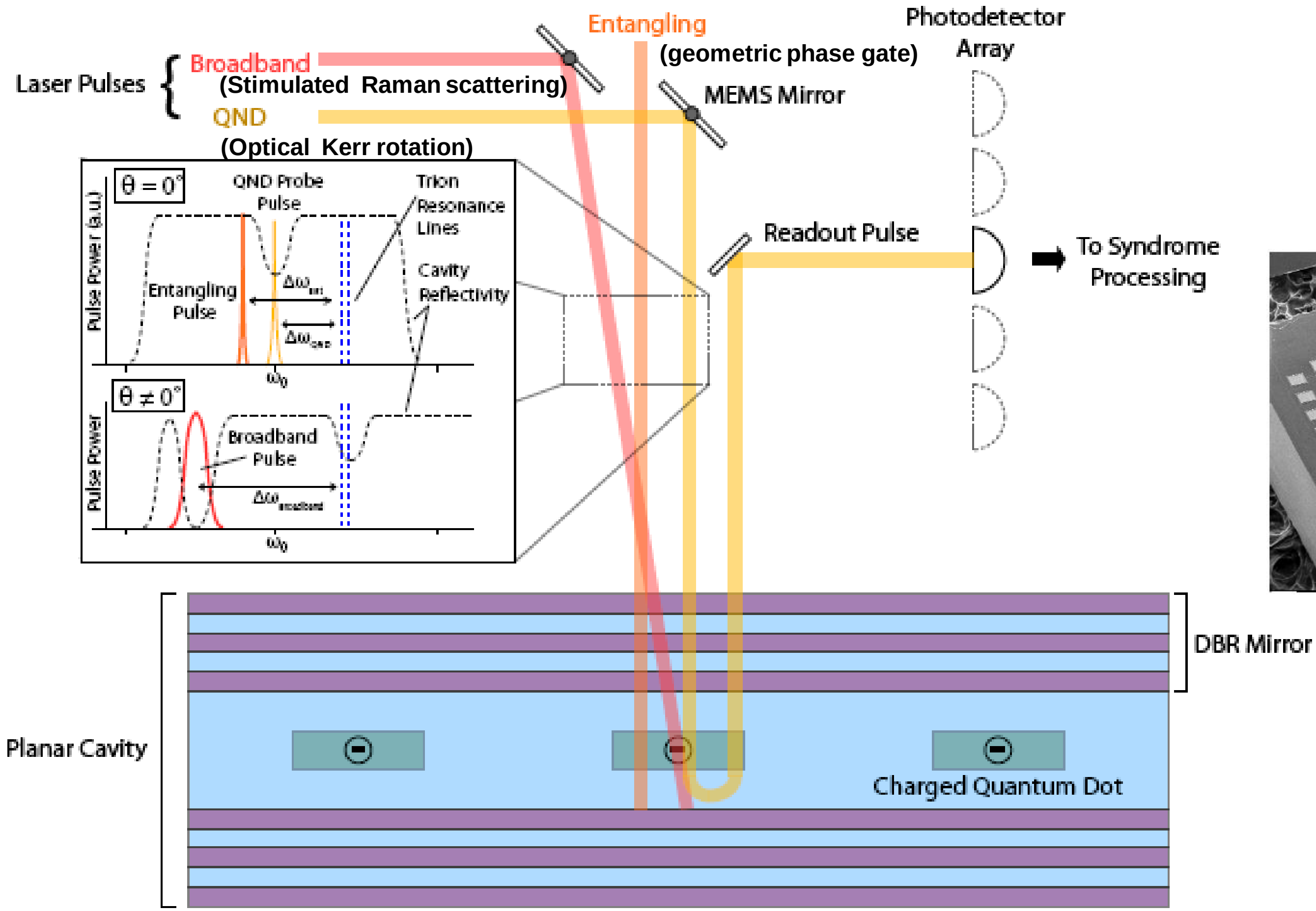

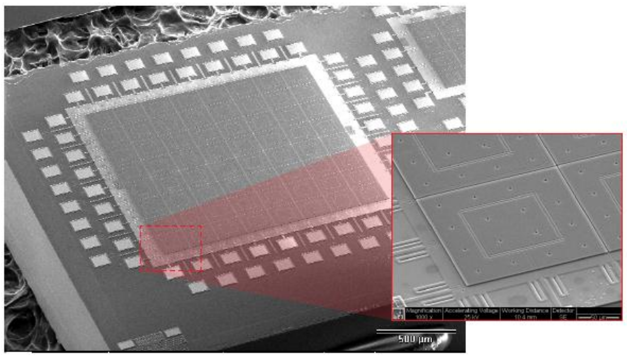

Proposal: PRL 99, 040501(2007), PRB 84, 235307(2011)
Electron spin: Nature 456, 218(2008), Nature Physics 4, 780(2008), Nature Photonics 4, 367(2010)
Hole spin: Nature physics 7, 872(2011)

Parameters for Layer 1: Quantum Operation

Operation	Mechanism	Duration	Notes
Spin phase precession ($\hat{Z}$-axis)	Magnetic field splitting of spin energy levels	$T_{\mathrm{Larmor}} = 40$ ps	Inhomogeneous nuclear environment causes spectral broadening in Larmor frequency, which is the source of $T_2{}^*$ processes.
Spin state rotation pulse	Stimulated Raman transition with broadband optical pulse	$\tau_{\mathrm{pulse}} =$ 4 ps	Red-detuned from spin ground state-trion transitions.
Entangling Operation	Nonlinear phase shift of spin states via coupling to a common cavity mode	$\tau_{\mathrm{entangle}} = 32$ ns	CW laser signal modulated by an electro-optic modulator (EOM).
QND Measurement	Dispersive phase-shift of light reflected from planar cavity	$\tau_{\mathrm{QND}} = 1$ ns	CW laser signal modulated by an EOM.

Virtual Layer

➢ *Cause destructive interference of systematic errors*

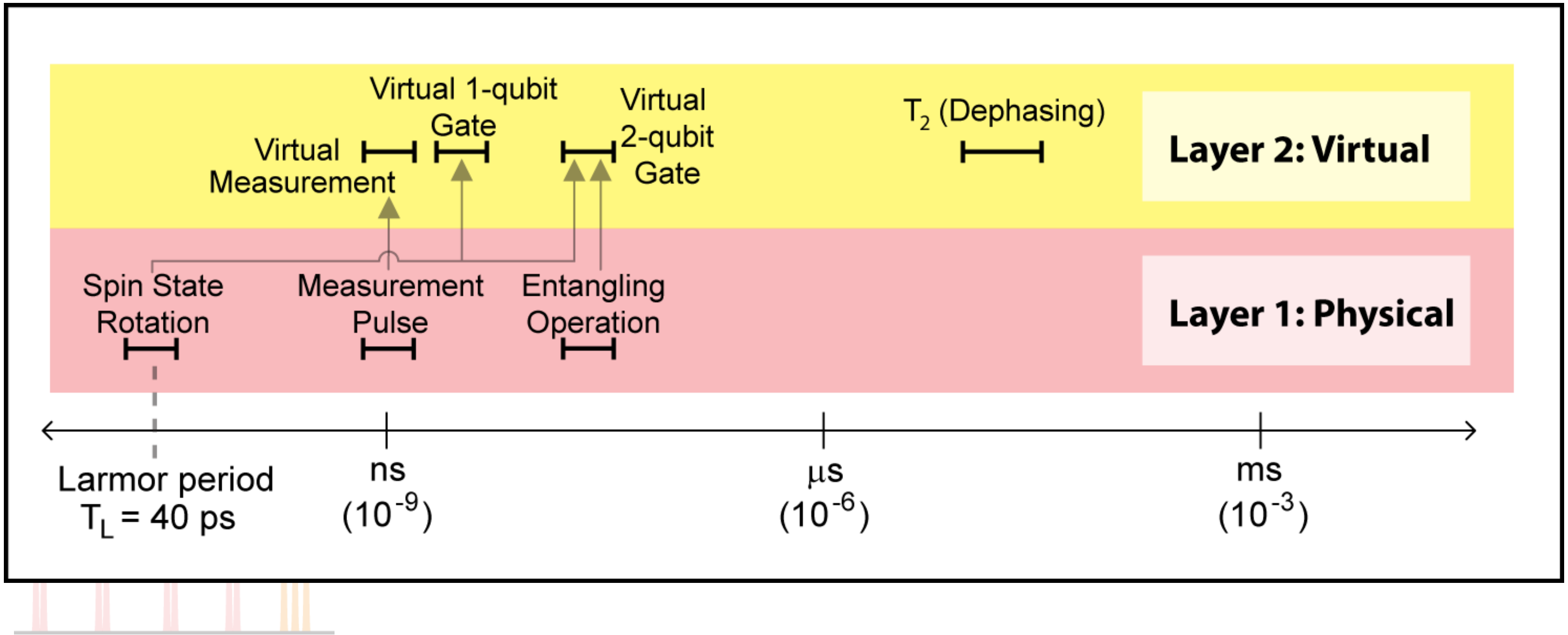

BB1 compensation sequence to correct gate errors, such as laser intensity fluctuations

- Wimperis, *J. Magn. Reson. Ser. B* **109**, 221 (1994)

Virtual Layer

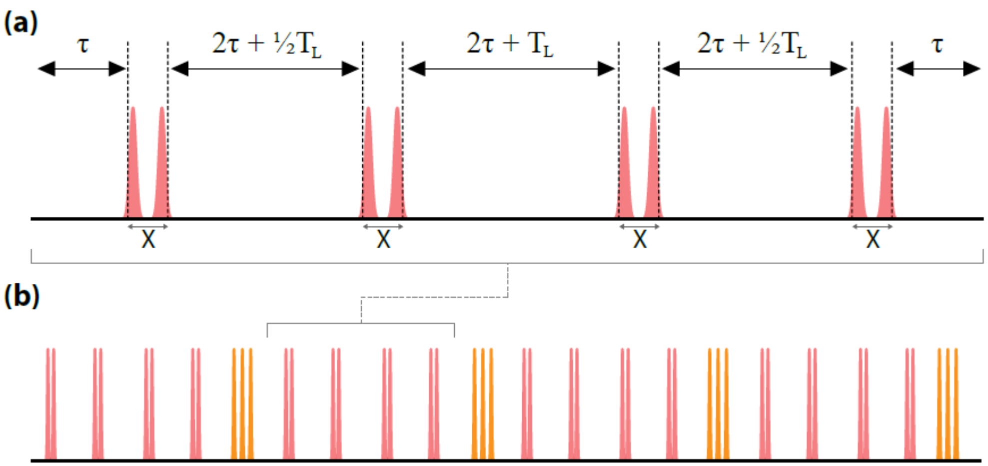

A special dynamical decoupling sequence for QuDOS, known as 8H since it requires eight Hadamard pulses. TL is the Larmor period determined by the external magnetic eld. (a) Timing specication for the 8H sequence, where is an arbitrary time. Each of the pulse pairs enacts a -rotation around the X-axis of the virtual qubit Bloch sphere. For 8H to work eciently, T2. (b) Four 8H sequences in a row interleaved with arbitrary gates formed from three Hadamard pulses (orange). The overall sequence forms a virtual gate by way of a BB1 compensation sequence.

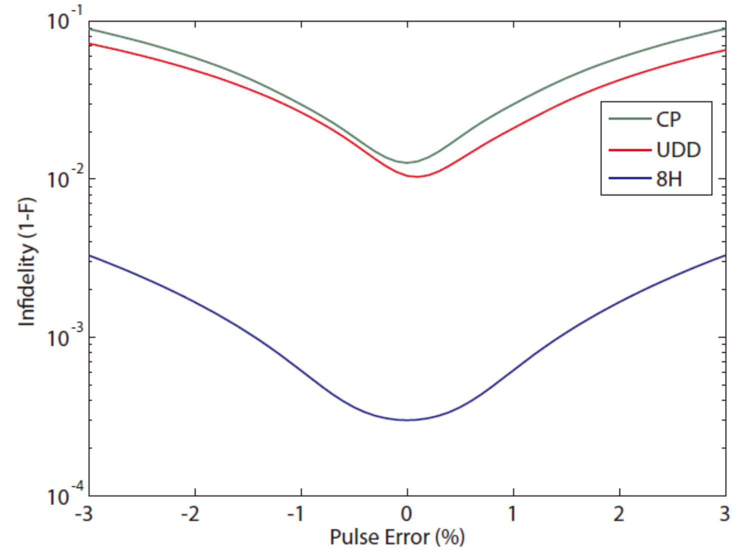

Simulation of the decoupling eectiveness of the 8H sequence compared to CP and UDD (each using 4 X gates) in the presence of dephasing noise and control errors. Here, “pulse error” is a systematic, relative deviation in the energy of every pulse. In all cases, two Hadamard pulses are combined to produce an approximate X gate. The vertical axis is indelity after evolution of the sequence in Fig. (a) with $\tau = 1$ ns; here indelity is 1 - F = 1 -χ II , whereχ II is the identity-to-identity matrix element in process tomography for the decoupling gate sequence with random noise. Since we aim to execute virtual gates with 1-F < 10^{-3}, laser pulse errors must be less than 1% in order for the virtual qubit memory error rate to be adequately low.

Optical Spin Echo Experiment with a Single Spin in Planar Microcavity

D. Press et al., Nature Photonics 4, 367 (2010)

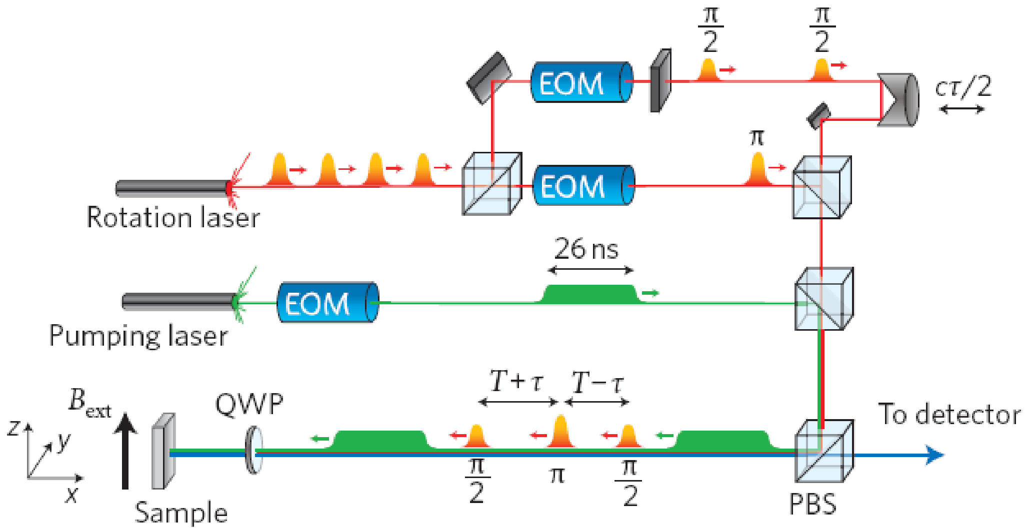

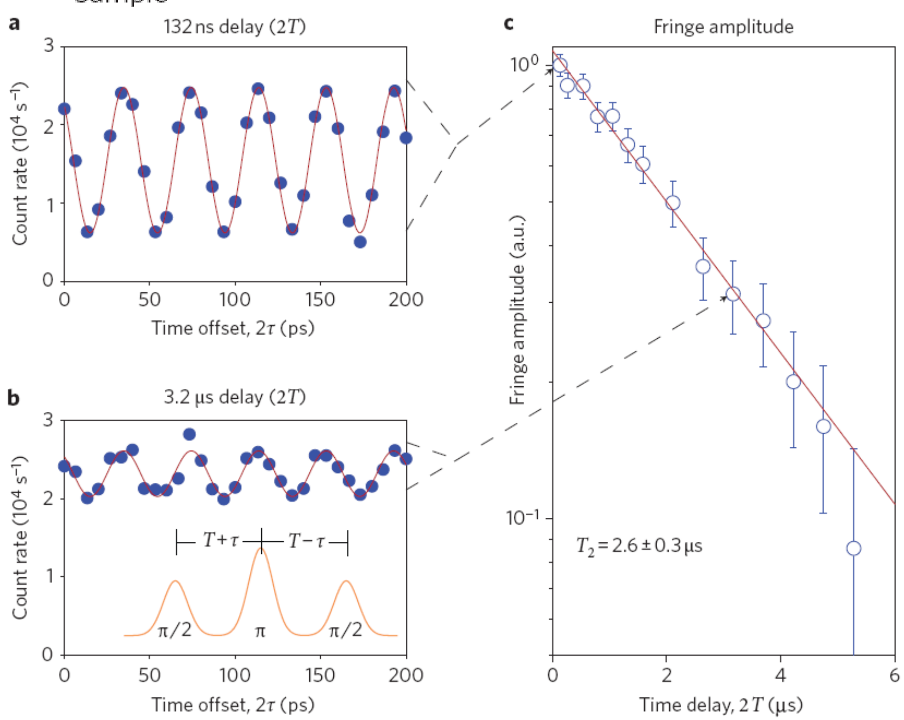

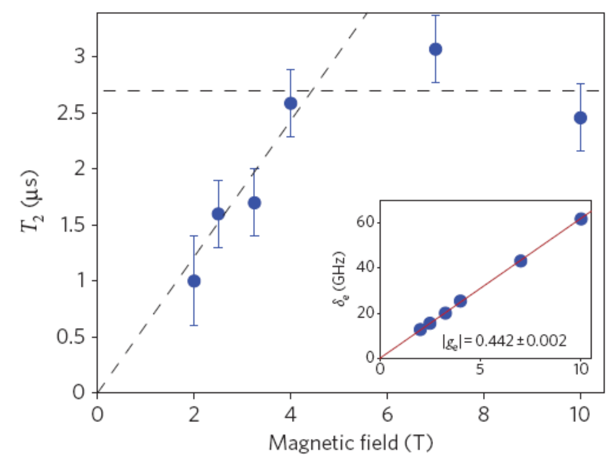

Shorter T_2 observed at B<4T
(⇨ paramagnetic impurity?)

Quantum Error Correction Layer

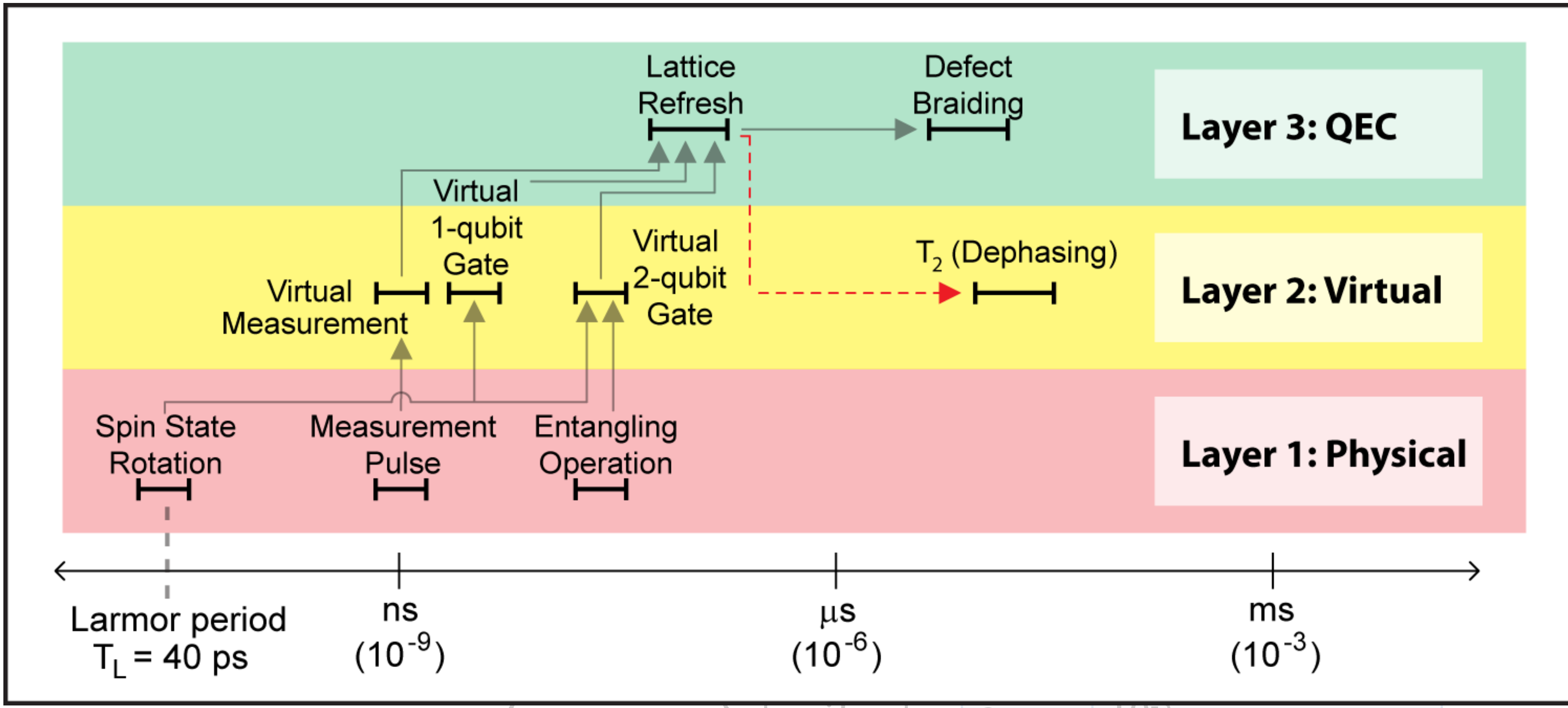

$$\epsilon_L \approx C \left(\frac{\epsilon_V}{\epsilon_{\mathrm{thresh}}} \right)^{[\ 2\ ]}$$

ε_V	10^{-3}
C	0.03
ε_L	10^{-15}
d	29

Fowler, *et al.* arXiv/1110.5133 (2011)

Topological Surface Code

Two advantages:

- High threshold for gate errors $\lesssim$ 1 %
- Requires only nearest-neighbor interaction

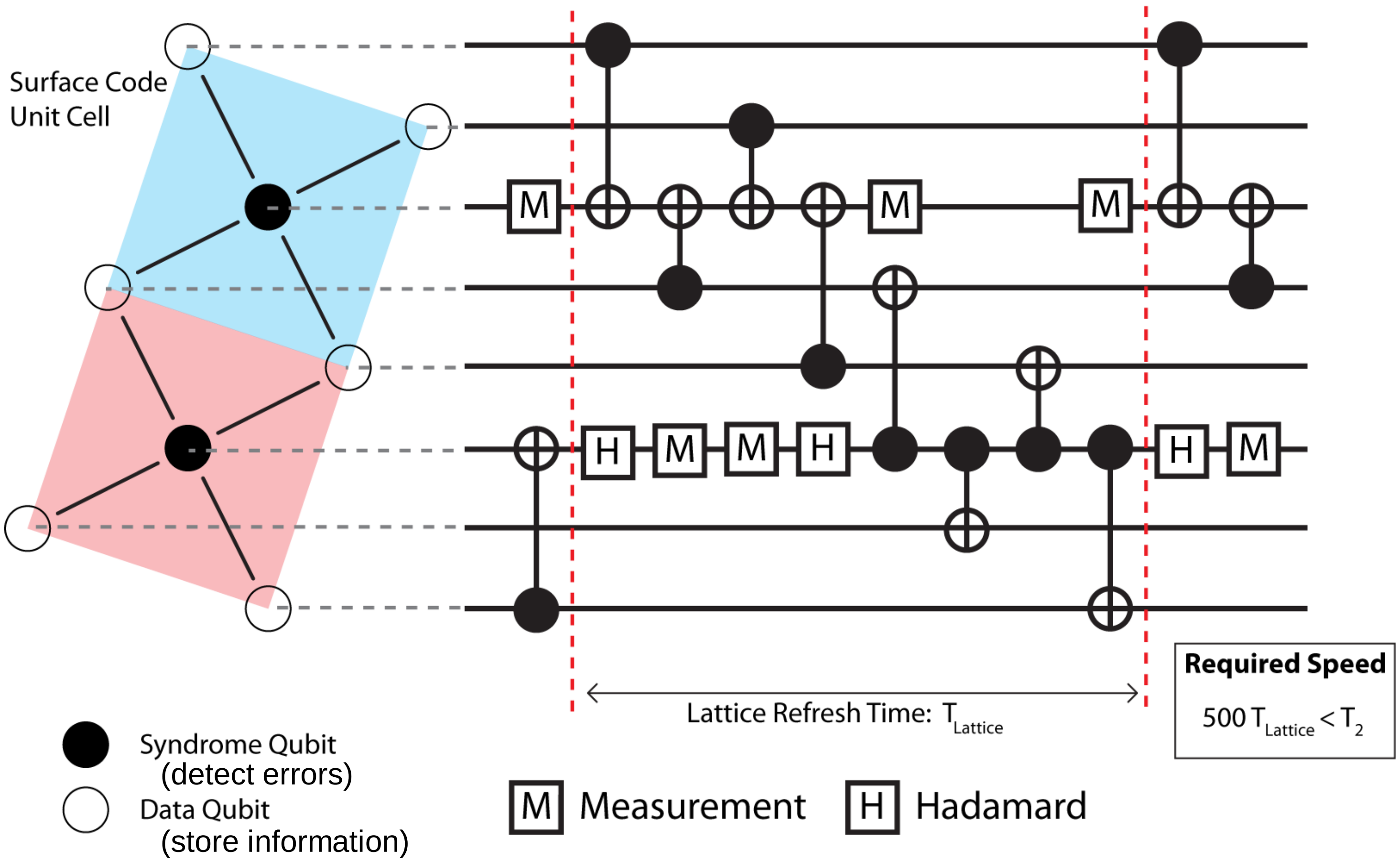

A lattice refresh cycle of the surface code can be performed in parallel across the entire 2D array of qubits.

Separation in Time Scales

- Operation times increase by orders of magnitude from Physical to Logical layer

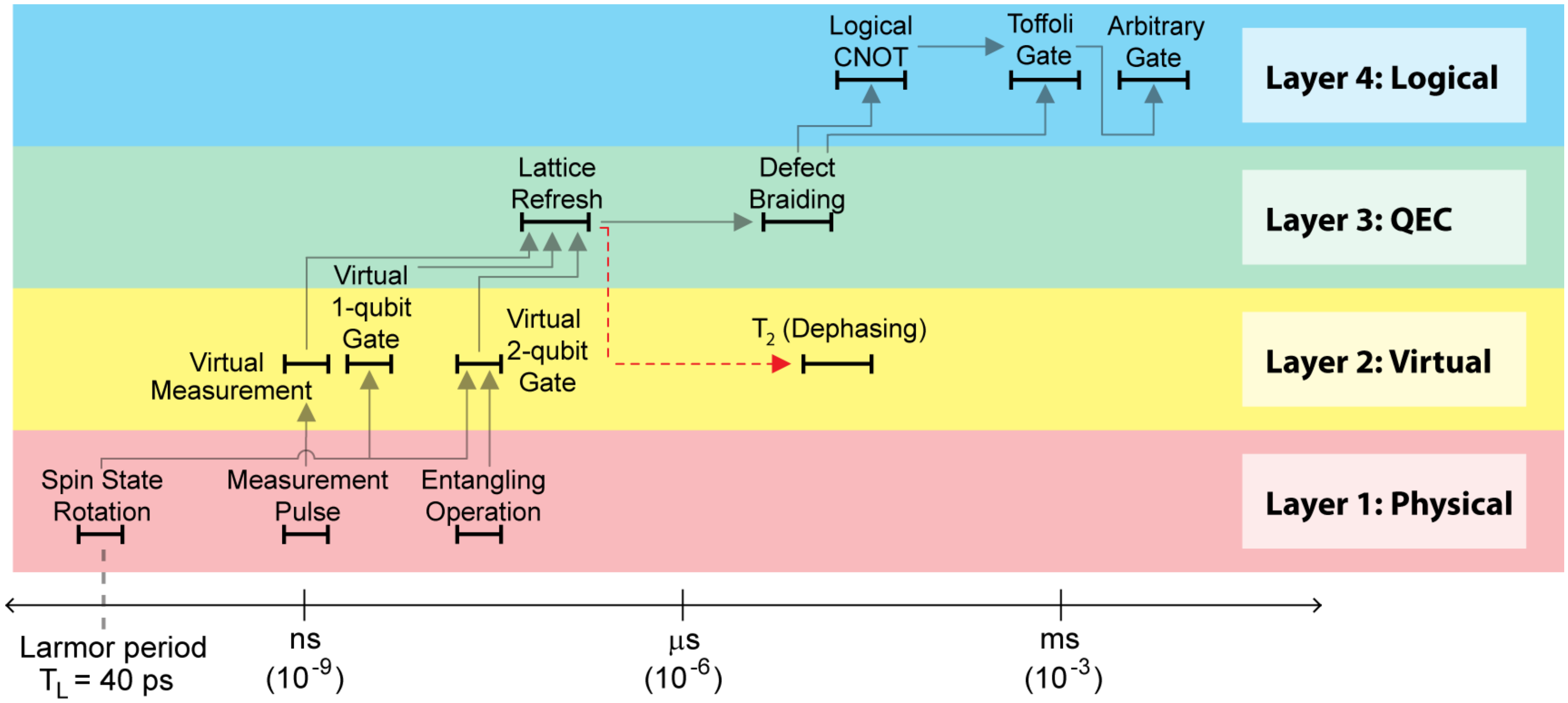

Primary Control Cycle of the Surface Code Quantum Computer – Pipelining –

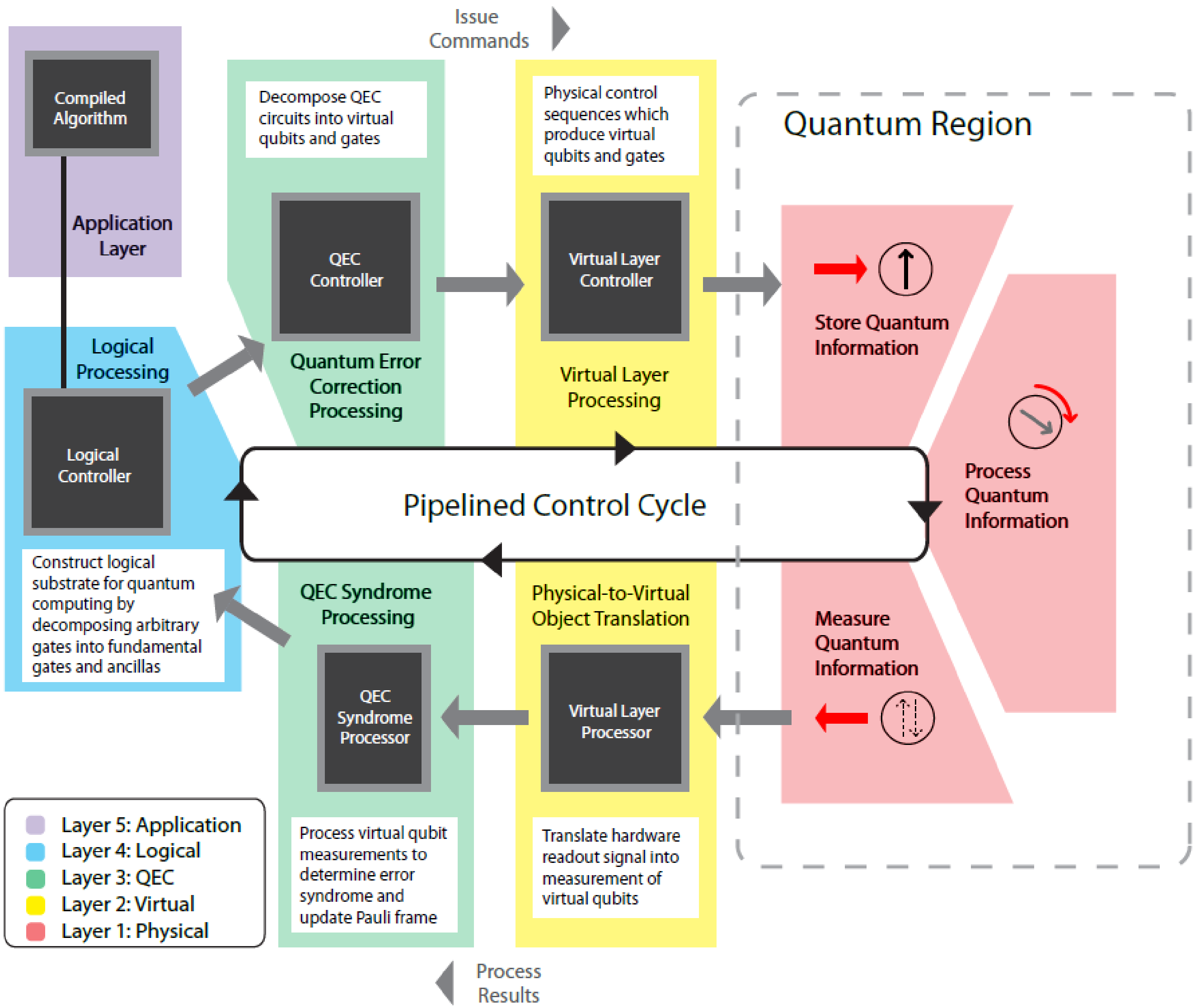

N. Cody Jones et al., arXiv:1010.5022 [quant-ph]

Resource and Operation Time of Surface Code Architecture

Shor's factoring algorithm for 2048-bit integer

Parameter	Symbol	Value
Threshold error per virtual gate	ϵ_{thresh}	7.5×10^{-3}
Error per virtual gate	ϵ_V	1×10^{-3}
Number of logical gates	K	9×10^{12}
Number of logical qubits	Q	12288
Error per logical gate	ϵ_L	9×10^{-20}
Surface code distance	d	53
Virtual qubits per logical qubit		19600

Operation	Label	Composition	Max Duration
Lattice Refresh with Alternating Phase Masks	LatticeRefresh	$2 \times$ (IZ · $4 \times$ CNOT · MZ · IX · $4 \times$ CNOT · MX)	1.61 μs
Defect Braiding	DefectBraid	$30 \times$ LatticeRefresh	48.4 μs
Logical CNOT	LogicalCNOT	$3 \times$ DefectBraid	145 μs
State Distillation	StateDistill	$5 \times$ DefectBraid	242 μs
Logical Toffoli Gate	LogicalToffoli	$14 \times$ DefectBraid	678 μs

# of logical qubits Q ~ 6N

Success probability of quantum algorithm

~99.99%

$\epsilon_L \leq 10^{-4}/KQ$

code distance 53

total number of physical qubits

2×10^8 (minimum)

~ 10^9 (sufficient)

Total computational time ~10 days

Circuit Depth Shor's Algorithm

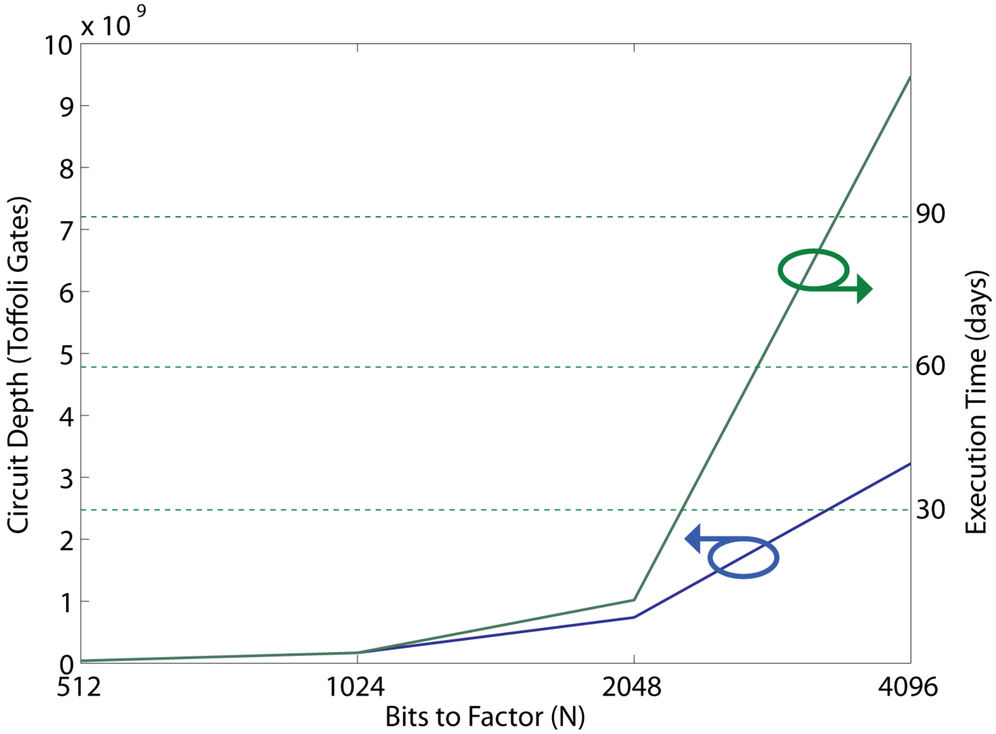

Assumptions
Optical quantum dots
Surface code QEC
Shor implementation given in [Van Meter, *et al. IJQI* **8**, 295 (2010)]
Fixed size: 10^5 logical qubits

- Algorithm stalls when distillation is not fast enough
- Require ~90% of QC devoted to distillation

量子誤り訂正コードで量子ビットを守る
− 過保護に育てられたひ弱な子供のように −